Post-buckling analysis of Mindlin Cut out-plate reinforced by FG-CNTs

Mohsen Motezaker[*1] and Arameh Eyvazian[2]

[1]School of Railway Engineering, Iran University of Science and Technology, Tehran, Iran
[2]Mechanical and Industrial Engineering Department, College of Engineering, Qatar University, P.O. Box 2713, Doha, Qatar

Abstract. In the present research post-buckling of a cut out plate reinforced through carbon nanotubes (CNTs) resting on an elastic foundation is studied. Material characteristics of CNTs are hypothesized to be altered within thickness orientation which are calculated according to Mori-Tanaka model. For modeling the system mathematically, first order shear deformation theory (FSDT) is applied and using energy procedure, the governing equations can be derived. With respect to Rayleigh-Ritz procedure as well as Newton-Raphson iterative scheme, the motion equations are solved and therefore, post-buckling behavior of structure will be tracked. Diverse parameters as well as their reactions on post-buckling paths focusing cut out measurement, CNT's volume fraction and agglomeration, dimension of plate and an elastic foundation are investigated. It is revealed that presence of a square cut out can affect negatively post-buckling behavior of structure. Moreover, adding nanocompsits in the matrix leads to enhancement of post-buckling response of system.

Keywords: post-buckling; rectangular cut out plate; FSDT; Newton-Raphson iterative technique; nanocomposite

1. Introduction

Undoubtedly, in spite of abundant researches and investigations as to detection of either rational ways or materials for strengthening the structures in various domains, reinforcing structures through nanocomposites have stood out since last decade. Nanocomposites such as CNTs and glass fibers have been reputed and popular materials to be added into structures for this intention. The mentioned material possesses properties containing enhancement in modulus, flexural strength and heat distortion temperature and so on and therefore, they have become usable materials in particular in various regions of engineering. Firstly, several researches have done investigating nanocomposite's properties and their advantages (Vinson 1999) and (Herman *et al.* 2005). Likewise, there are numerous papers studying behavior of nanocomposite structures. Asghar *et al.* (2020) studied frequency of double walled carbon nanotubes (DWCNTs). Effects of different boundary conditions as well as forces among internal and external tubes named van der waals have been analyzed. Gengele *et al.* (2018) carried out buckling of both DWCNTs and single walled carbon nanotubes (DWCNTs) placed vertically. In addition, influence of van der waals force has been explored. They illustrated that modulus of such CNTs raises while the size rises. In another work, bending evaluation of CNTs surrounded by elastic foundation has been reported by Akgoz and Civalek (2016). Using energy method and modified strain gradient theory, governing equation were obtained and solved by Navier procedure. Wave dispersion of DWCNTs was discussed by Gul and Aydogdu (2017). It has been mentioned that through Doublet Mechanics wave dispersion was studied which had precise outcomes for flexural as well as axial wave dispersion in nanotubes. Moreover, the effect of van der waals has been taken into consideration.

Regardless of CNTs, there are numerable researches in which other nanocomposites and their static as well as dynamic behaviors have been investigated owing to a wide range of applications in diverse scientific clusters specifically in engineering. Karimiasl *et al.* (2020) analyzed frequency of polymer-graphene platelet-fiber (GPF) besides CNTs in hygrothermal environment.. In this paper, different distributions of nanocomposites, temperature influence and curvature proportion have been analyzed as well. Oktem and Adali (2018) carried out of buckling of columns made up of polymer/clay nanocomposite. In this research, elastic coefficients of nanocomposite are obtained utilizing micromechanical meyhod. Furthermore, influence of uncertain material characteristics are analyzed. Moradi-Dastjerdi and Behdinan (2020) explored stability of a sandwich with polymeric porous core as well as graphene/polymer nanocomposite face sheets. Due to presence of such a face sheets, the structure turns into a multifunctional sandwich plate. They ascertained that using graphene considerably enhances the whole stability of sandwich structure.

Reinforcing agents are regarded as one of the essential capability of nanocomposites which give the structure strength and toughness. As a matter of fact, accurately putting nanocomposites into matrix results in improvement in the performance of structure significantly. As mentioned,

---

*Corresponding author, Ph.D.
E-mail: mohsen.motezaker@gmail.com

nano particles such as CNTs, grapheme and glass fibers are employed as reinforcements for fabricating strict polymer nanocomposites for sensitive usages. Qin *et al.* (2019) explored vibration of a shallow shell which has been reinforced by graphene platelets (GPLs). Influence of weight fractions of GPLs improving the frequency and subsequently stiffness of structure besides various edge conditions were investigated. Likewise, Liu *et al.* (2019) studied bending and vibration of annular plates reinforced via GPLs. Motion equations were obtained using energy method and solved utilizing differential quadrature method (DQM). For achieving efficient materials properties of GPLs, micromechanical model has been used and five various dispersions of GPLs were studied in which GPL-X possessed the best performance for the structure. Yang et al. (2017) investigated nonlinear dynamic of a microbeam reinforced through CNTs integrated by two piezoelectric layers. Damping influence, thermal environment as well as voltage were considered. In addition, pull-in instability of this structure was analyzed and they proved that pull-in voltage of sandwich plate considering damping system would be higher than other states. Kolahdouzan *et al.* (2018) carried out buckling and vibration of a microplate reinforced with CNTs incorporated by piezoelectric face sheets. Further, the sandwich structure is under two dimensional magnetic field and bi-axial loads. The results showed that using CNTs as reinforcing mean leads to increase in critical buckling load and natural frequency to a large extent. In another paper, two dimensional wave distribution of rotating nanobeam which is reinforced by porous material was investigated by Faroughi *et al.* (2019). General nonlocal theory has been utilized for gaining propagations of waves. Moreover, material variations as well as porosity were analyzed.

Post-buckling behavior in some cases known as the malformation after buckle inception, is able to reveal how a structure is going to fail while the force becomes so much. To put it differently, post-buckling response defines nonlinear behavior happening in a fraction of second. The first inception of is relevant to the mode shapes reached by a modal frequency evaluation. Further, post-buckling analysis is vital for guarantee safety of thin structures subjected to high loadings, energy absorbers as well as impact structures. Ninh (2018) analyzed post-buckling of cylindrical shell reinforced via CNTs incorporated with piezoelectric face sheets. Effects of different dispersions of nanocomposites, thermal environment and elastic foundation on torsional post-buckling response were considered and governing equations have been solved by Galerkin's method. Kolahchi *et al.* (2019) carried out post-buckling of imperfect graphene sheets in hygrothermal environment considering movable edge conditions. Further, the structure was under magnetic field. The governing equations were obtained by higher order shear deformation theory (HSDT) and solved with DQM. The imperfection included single and double vacancies and Stone-Wales. They ascertained that increment of imperfect degree can lead to decrease in buckling load. Akbas (2019) investigated post-buckling of a beam reinforced by fiber containing crack. In this work, fiber's volume fraction, its orientation

angles and crack depth were analyzed and shown that the mentioned parameters play important role in the post-buckling behavior of beam. Exploring post-buckling response of FGM sandwich structure exposed to mechanical compressive load was done by Do and Lee (2018). HSDT was used for formulation and solved using Newton-Raphson iterative scheme. It should be noticed that detective state was analyzed and determined that possesses important role in the post-buckling of sandwich structure. Wang *et al.* (2019) investigated post-buckling of steel columns which were prestressed. Furthermore, the optimistic length for the column was obtained.

To date, encouraged by these considerations, there is no paper investigating post-buckling behavior of a cut out plate reinforced through CNTs resting on Winkler-Pasternak medium. Further, the plate is subjected to biaxial compressive force. So as to obtain the governing equations, firstly, FSDT is employed and secondly, using domain decomposition as well as Rayleigh-Ritz procedure along with Newton-Raphson iterative scheme, plate's post-buckling behavior will be achieved. Effects of several essential variables includingcut out measurements, CNTs volume fraction, plate's aspect ratio and coefficients of surrounding medium upon post-buckling response of plate will be presented.

2. Problem definition

In order to show formation of a cut out plate reinforced through CNTs resting on an elastic foundation and under biaxial loads and magnetic field, Fig. 1 is illustrated. Further, a, b, d and h respectively represent length, width, length of square hole and total thickness of structure.

2.1 FSDT

In present research, Mindlin plate theory is employed for modelling the plate mathematically as below

$$u\left(x,y,z\right)=u_0\left(x,y\right)+z\,\phi_1\left(x,y\right), \qquad (1a)$$

$$v\left(x,y,z\right)=v_0\left(x,y\right)+z\,\phi_2\left(x,y\right), \qquad (1b)$$

$$w(x,y,z)=w_0(x,y), \qquad (1c)$$

in which u_0, v_0 and w_0 respectively describe mid-plane displacements in longitudinal, transverse and thickness directions. In addition, ϕ_1 as well as ϕ_2 express rotations around longitudinal and transverse orientations.

2.2 Material properties of nanocomposite plate

In present part, micromechanical procedure has been employed for material properties of nanocomposite plate.

Hence, concrete column's efficient modulus reinforced with SiO$_2$ nanoparticles will be enhanced. Based on (Mori and Tanaka 1973) there are various procedures achieving average characteristics of composite materials. It is clear because of easiness as well as resolution both at inclusion's low and high volume fraction Mori-Tanaka procedure (Mori and Tanaka 1973) will be utilized.

It should be mentioned that matrix is presumed isotropic and elastic and therefore E_m and υ_m represent Young's modulus the Poisson's ratio, respectively. The fundamental relations of composite materials for the stresses can be given by (Mori and Tanaka 1973)

$$\begin{Bmatrix} \sigma_{11} \\ \sigma_{22} \\ \sigma_{33} \\ \sigma_{23} \\ \sigma_{13} \\ \sigma_{12} \end{Bmatrix} = \begin{bmatrix} k+m & l & k-m & 0 & 0 & 0 \\ l & n & l & 0 & 0 & 0 \\ k-m & l & k+m & 0 & 0 & 0 \\ 0 & 0 & 0 & p & 0 & 0 \\ 0 & 0 & 0 & 0 & m & 0 \\ 0 & 0 & 0 & 0 & 0 & p \end{bmatrix} \begin{Bmatrix} \varepsilon_{11} \\ \varepsilon_{22} \\ \varepsilon_{33} \\ \gamma_{23} \\ \gamma_{13} \\ \gamma_{12} \end{Bmatrix} \tag{2}$$

In the above relation, σ_{ij}, ε_{ij} and γ_{ij} respectively define the stress and strain constituents. Further, k, m, n, l and p represent plane-strain bulk modulus, shear moduli in planes normal, modulus of uniaxial tension in x direction of the fiber, related cross modulus and shear moduli parallel to the fiber direction. So as to expand the above parameters and considering Mori-Tanaka model, they are defined as follow

$$k = \frac{E_m\{E_m c_m + 2k_r(1+v_m)[1+c_r(1-2v_m)]\}}{2(1+v_m)[E_m(1+c_r-2v_m)+2c_m k_r(1-v_m-2v_m^2)]}$$

$$l = \frac{E_m\{c_m v_m[E_m + 2k_r(1+v_m)]+2c_r l_r(1-v_m^2)]\}}{(1+v_m)[E_m(1+c_r-2v_m)+2c_m k_r(1-v_m-2v_m^2)]}$$

$$n = \frac{E_m^2 c_m(1+c_r-c_m v_m)+2c_m c_r(k_r n_r-l_r^2)(1+v_m)^2(1-2v_m)}{(1+v_m)[E_m(1+c_r-2v_m)+2c_m k_r(1-v_m-2v_m^2)]}$$

$$+ \frac{E_m[2c_m^2 k_r(1-v_m)+c_r n_r(1+c_r-2v_m)-4c_m l_r v_m]}{E_m(1+c_r-2v_m)+2c_m k_r(1-v_m-2v_m^2)} \tag{3}$$

$$p = \frac{E_m[E_m c_m + 2p_r(1+v_m)(1+c_r)]}{2(1+v_m)[E_m(1+c_r)+2c_m p_r(1+v_m)]}$$

$$m = \frac{E_m[E_m c_m + 2m_r(1+v_m)(3+c_r-4v_m)]}{2(1+v_m)\{E_m[c_m+4c_r(1-v_m)]+2c_m m_r(3-v_m-4v_m^2)\}}$$

It should be noted that subscripts m and r express respectively matrix and reinforcement. c_m and c_r describe respectively matrix's volume fractions and nanoparticles. Moreover, k_r, l_r, n_r, p_r and m_r describe reinforcing phase for the composite material's Hill's elastic moduli (Mori and Tanaka 1973).

2.3 Energy principle

Strain energy for composite structure can be written as

$$U = \frac{1}{2}\int_A \int_{-\frac{h}{2}}^{\frac{h}{2}} \left(\sigma_{xx}\varepsilon_{xx} + \sigma_{yy}\varepsilon_{yy} + \sigma_{yz}\gamma_{yz} + \sigma_{xz}\gamma_{xz} \right.$$
$$\left. + \sigma_{xy}\gamma_{xy} \right) dz dA . \tag{4}$$

With respect to Hook law, the stress-strain relation can be given by

$$\sigma_{ij} = C : \varepsilon_{ij} , \tag{5}$$

Utilizing Eq. (5), constitutive correlation for the stresses of a nanocomposite structure can be expressed as

$$\begin{Bmatrix} \sigma_{xx} \\ \sigma_{yy} \\ \sigma_{yz} \\ \sigma_{xz} \\ \sigma_{xy} \end{Bmatrix} = \begin{bmatrix} Q_{11} & Q_{12} & 0 & 0 & 0 \\ & Q_{22} & 0 & 0 & 0 \\ & & Q_{44} & 0 & 0 \\ & & & Q_{55} & 0 \\ sym. & & & & Q_{66} \end{bmatrix} \begin{Bmatrix} \varepsilon_{xx} \\ \varepsilon_{yy} \\ \gamma_{yz} \\ \gamma_{xz} \\ \gamma_{xy} \end{Bmatrix}, \tag{6}$$

Further, $Q_{ij} (i, j = 1, 2, ..., 6)$ is written as below

$$Q_{11} = \frac{E_{11}}{1-\upsilon_{12}\upsilon_{21}} ? Q_{22} = \frac{E_{22}}{1-\upsilon_{12}\upsilon_{21}}, Q_{12} = \frac{\upsilon_{21}E_{11}}{1-\upsilon_{12}\upsilon_{21}} ?$$
$$Q_{44} = G_{23}, Q_{55} = G_{13}, Q_{66} = G_{12}. \tag{7}$$

The specific strain components regarding strain-displacement correlations based on von-Karman are described as below

$$\begin{Bmatrix} \varepsilon_{xx} \\ \varepsilon_{yy} \\ \gamma_{yz} \\ \gamma_{xz} \\ \gamma_{xy} \end{Bmatrix} = \begin{Bmatrix} \varepsilon_{xx}^0 \\ \varepsilon_{yy}^0 \\ \gamma_{yz}^0 \\ \gamma_{xz}^0 \\ \gamma_{xy}^0 \end{Bmatrix} + z \begin{Bmatrix} \varepsilon_{xx}^1 \\ \varepsilon_{yy}^1 \\ \gamma_{yz}^1 \\ \gamma_{xz}^1 \\ \gamma_{xy}^1 \end{Bmatrix}, \tag{8}$$

where

$$\begin{Bmatrix} \varepsilon_{xx}^0 \\ \varepsilon_{yy}^0 \\ \gamma_{yz}^0 \\ \gamma_{xz}^0 \\ \gamma_{xy}^0 \end{Bmatrix} = \begin{Bmatrix} \dfrac{\partial u_0}{\partial x} \\ \dfrac{\partial v_0}{\partial y} \\ \dfrac{\partial w_0}{\partial y} + \phi_2 \\ \dfrac{\partial w_0}{\partial x} + \phi_1 \\ \dfrac{\partial u_0}{\partial y} + \dfrac{\partial v_0}{\partial x} \end{Bmatrix}, \tag{9}$$

$$\begin{Bmatrix} \varepsilon_{xx}^1 \\ \varepsilon_{yy}^1 \\ \gamma_{yz}^1 \\ \gamma_{xz}^1 \\ \gamma_{xy}^1 \end{Bmatrix} = \begin{Bmatrix} \dfrac{\partial \phi_1}{\partial x} \\ \dfrac{\partial \phi_2}{\partial y} \\ 0 \\ 0 \\ \dfrac{\partial \phi_1}{\partial x} + \dfrac{\partial \phi_2}{\partial y} \end{Bmatrix}. \tag{10}$$
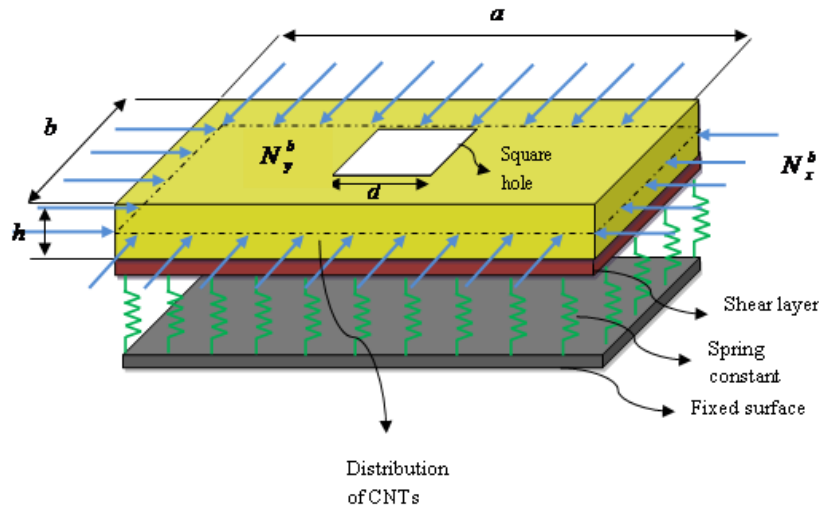
Fig. 1 Configuration of cut out plate resting on elastic medium

In the next step, stress consequences containing N_{ij}^{nl}, M_{ij}^{nl} and Q_k^{nl} can be written as

$$\begin{Bmatrix} N_{xx} \\ N_{yy} \\ N_{xy} \end{Bmatrix} = \int_{-\frac{h}{2}}^{\frac{h}{2}} \begin{Bmatrix} \sigma_{xx} \\ \sigma_{yy} \\ \sigma_{xy} \end{Bmatrix} dz ,$$

(11)

$$\begin{Bmatrix} M_{xx} \\ M \\ M_{xy} \end{Bmatrix} = \int_{-\frac{h}{2}}^{\frac{h}{2}} z \begin{Bmatrix} \sigma_{xx} \\ \sigma_{yy} \\ \sigma_{xy} \end{Bmatrix} dz ,$$

(12)

$$\begin{Bmatrix} Q_y \\ Q_x \end{Bmatrix} = \kappa_s \int_{-\frac{h}{2}}^{\frac{h}{2}} \begin{Bmatrix} \sigma_{yz} \\ \sigma_{xz} \end{Bmatrix} dz ,$$

(13)

in which k_s illustrates the coefficient of transverse shear correction. For expansion of the constitutive correlations, Eq. (5) as well as Eqs. (11)-(13) can be utilized as follow

$$N_{xx} = A_{11}\frac{\partial u_0}{\partial x} + B_{11}\frac{\partial \phi_1}{\partial x} + A_{12}\frac{\partial v_0}{\partial y} + B_{12}\frac{\partial \phi_2}{\partial y},$$

(14)

$$N_{yy} = A_{12}\frac{\partial u_0}{\partial x} + B_{12}\frac{\partial \phi_1}{\partial x} + A_{22}\frac{\partial v_0}{\partial y} + B_{22}\frac{\partial \phi_2}{\partial y},$$

(15)

$$N_{xy} = A_{66}\frac{\partial}{\partial x}v_0 + B_{66}\frac{\partial}{\partial x}\phi_2 + A_{66}\frac{\partial}{\partial y}u_0 + B_{66}\frac{\partial}{\partial y}\phi_1,$$

(16)

$$M_{xx} = B_{11}\frac{\partial}{\partial x}u_0 + D_{11}\frac{\partial}{\partial x}\phi_1 + B_{12}\frac{\partial}{\partial y}v_0 + D_{12}\frac{\partial}{\partial y}\phi_2,$$

(17)

$$M_{yy} = B_{12}\frac{\partial}{\partial x}u_0 + D_{12}\frac{\partial}{\partial x}\phi_1 + B_{22}\frac{\partial}{\partial y}v_0 + D_{22}\frac{\partial}{\partial y}\phi_2,$$

(18)

$$M_{xy} = B_{66}\frac{\partial}{\partial x}v_0 + D_{66}\frac{\partial}{\partial x}\phi_2 + B_{66}\frac{\partial}{\partial y}u_0 + D_{66}\frac{\partial}{\partial y}\phi_1,$$

(19)

$$Q_{xz} = \kappa_s A_{55}\frac{\partial}{\partial x}w_0 + \kappa_s A_{55}\phi_1,$$

(20)

$$Q_{yz} = \kappa_s A_{44}\frac{\partial}{\partial y}w_0 + \kappa_s A_{44}\phi_2.$$

(21)

In the above formulations, stiffness constituents are given by

$$\left(A_{ij}, B_{ij}, D_{ij}\right) = \int_{-\frac{h}{2}}^{\frac{h}{2}} Q_{ij}(z)\left(1, z, z^2\right) dz .$$

(22)

Hence

$$U = \frac{1}{2}\int_A \left(N_{xx}\left(\frac{\partial}{\partial x}u_0\right) + M_{yy}\frac{\partial}{\partial y}\phi_2 \right.$$

$$+ N_{yy}\left(\frac{\partial}{\partial y}v_0\right) + M_{xx}\frac{\partial}{\partial x}\phi_1$$

$$+ N_{xy}\left(\frac{\partial u_0}{\partial y} + \frac{\partial v_0}{\partial x}\right) + Q_x\left(\frac{\partial}{\partial x}w_0 + \phi_1\right)$$

$$\left. + M_{xy}\left(\frac{\partial}{\partial y}\phi_1 + \frac{\partial}{\partial x}\phi_2\right) + Q_y\left(\frac{\partial}{\partial y}w_0 + \phi_2\right)\right) dA.$$

(23)

As shown in the Fig. 1, the structure is subjected to exterior forces including biaxial compressive loads, elastic foundation and longitudinal magnetic field.

Based on Fig. 1, the structure is under biaxial loading ($N_x^b = -F$ and $N_y^b = -kF$); hence, work done for compressive load can be obtained as follow

$$W_b = -\frac{1}{2}\int_A \left(N_x^b\left(\frac{\partial}{\partial x}w(x,y)\right)^2 + N_y^b\left(\frac{\partial}{\partial y}w(x,y)\right)^2\right) dA .$$

(24)

Furthermore, the structure is rested on elastic foundation and consequently work done by the foundation is written as follow

$$W_f = -\int_A \left(K_w w - G_p\nabla^2 w \right) w\, dA,$$

(25)

in which K_w and G_p define respectively Winkler's spring coefficient and shear medium parameter.
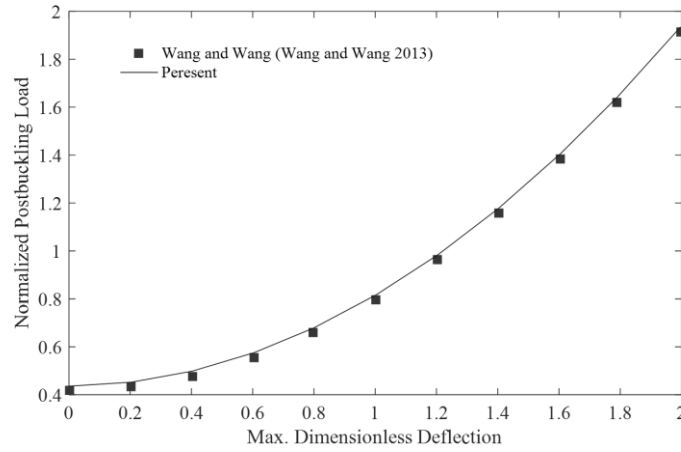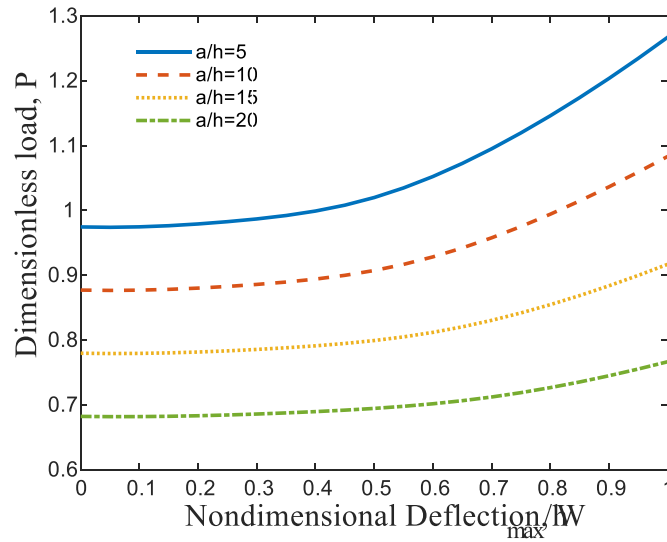
Fig. 2 Collation of post-buckling load for plate

Fig. 3 The effect of aspect ratio on non-dimensional post-buckling load

Finally, the structure's total energy may be written as

$$
\Pi = \int_A \left\{ \frac{1}{2}\left[N_{xx}\left(\frac{\partial}{\partial x}u_0\right) + N_{yy}\left(\frac{\partial}{\partial y}v_0\right) \right. \right.
$$
$$
+ N_{xy}\left(\frac{\partial u_0}{\partial y} + \frac{\partial v_0}{\partial x}\right) + M_{xx}\frac{\partial}{\partial x}\phi_1 + M_{yy}\frac{\partial}{\partial y}\phi_2
$$
$$
\left. + M_{xy}\left(\frac{\partial}{\partial y}\phi_1 + \frac{\partial}{\partial x}\phi_2\right) + Q_x\left(\frac{\partial}{\partial x}w_0 + \phi_1\right) + Q_y\left(\frac{\partial}{\partial y}w_0 + \phi_2\right) \right]
$$
$$
\left. + \frac{1}{2}\left[N_x^b\left(\frac{\partial}{\partial x}w\right)^2 + N_y^b\left(\frac{\partial}{\partial y}w\right)^2 \right] + \left[\left(K_w w - G_p\nabla^2 w\right)w\right] \right\}dA. \quad (26)
$$

3. Solution method

Displacement quantities for rectangular plate and simply supported state are written as follow

$$
w_0(x,y) = w_{mn}\,sin\left(\frac{m\pi x}{a}\right)sin\left(\frac{n\pi y}{b}\right), \quad (27)
$$

$$
\phi_1(x,y) = \phi_{1mn}\,cos\left(\frac{m\pi x}{a}\right)sin\left(\frac{n\pi y}{b}\right), \quad (28)
$$

$$
\phi_2(x,y) = \phi_{2mn}\,sin\left(\frac{m\pi x}{a}\right)cos\left(\frac{n\pi y}{b}\right), \quad (29)
$$

where m as well as n represent mode numbers and $\{w_{mn}, \phi_{1mn}, \phi_{2mn}\}$ demonstrate amplitudes. Introducing Eqs. (27)-(29) to Eq. (26), following formulation will be derived

$$
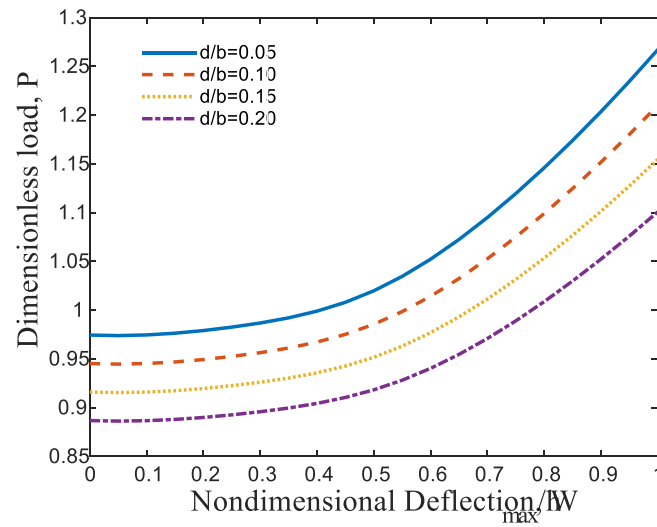\left(K - FK_G\right)d = 0, \quad (30)
$$

Fig. 4 The influence of magnitude of square cut out on non-dimensional post-buckling load
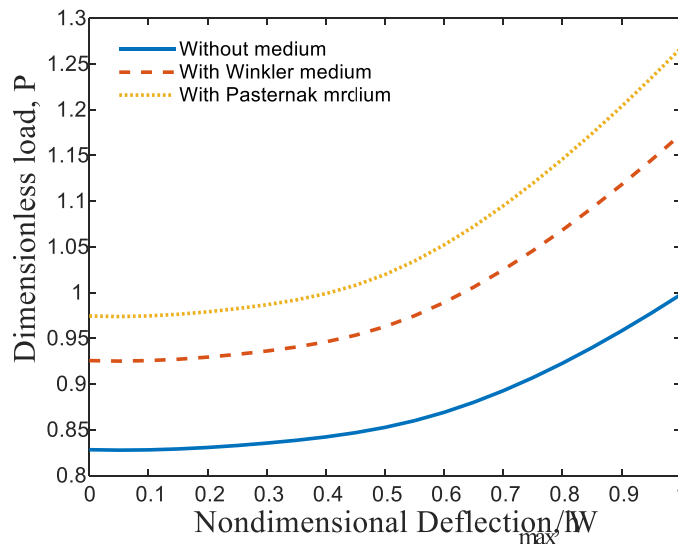

Fig. 5 Influence of elastic medium on the non-dimensional post-buckling load

in which K and K_G define respectively linear stiffness matrix and geometric stiffness matrix. F expresses post-buckling load and d would be equivalent to $\{w_{mn}, \phi_{1mn}, \phi_{2mn}\}^T$. Eventually, structure's post-buckling reply will be achieved utilizing Eq. (30) through Rayleigh-Ritz method as well as Newton-Raphson iterative technique.

4. Numerical results

A plate cut out on its central region reinforced by CNTs resting on an elastic foundation is considered and post-buckling response of this structure will be studied in this section. In order to spread this investigation effect of

several variables including cut out measurement, CNT's volume fraction and structure's aspect ratio are analyzed. Likewise, influence of exterior factors such as elastic foundation, biaxial compressive load and magnetic field on post-buckling response of structure are investigated. It should be noticed that Young's modulus and Poisson's ratio of this plate are $E^m = 2.1(GPa)$ and $\upsilon_m = 0.34$,respectively.

To date, there is no paper published in which post-buckling response of a cut out plate reinforced by CNTs is carried out. Therefore, for discussion of the outcomes and accuracy of present paper with other researches, we compare the obtained result for post-buckling behavior of this plate with (Wang and Wang 2013) plotted in Fig. 2. As seen, in this figure post-buckling load with regard to utmost
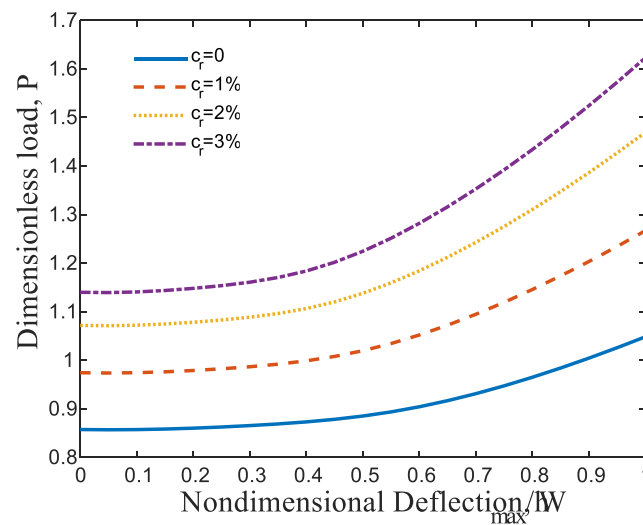
Fig. 6 The influence of different CNTs volume fraction on non-dimensional post-buckling load
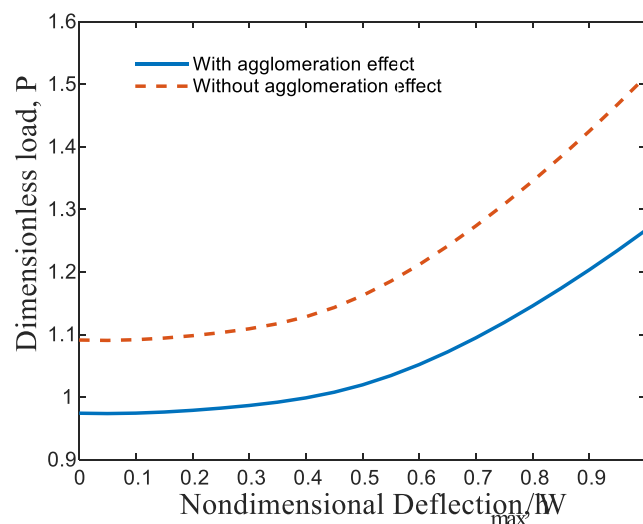

Fig. 7 The effect of agglomeration of   CNTs on non-dimensional post-buckling load

deflection is illustrated. It is vivid that derived outcomes is in a good accordance with the results obtained by (Wang and Wang 2013).

Fig.3 illustrates influence of plate's aspect ratio upon non-dimensional post-buckling load with regard to non-dimensional amplitude of deflection.

As can be seen, the more length and subsequently aspect ratio of plate raises, the more non-dimensional post-buckling load of plate is reduced. It can be justified by this reason that increase in length of structure causes decrease in stiffness of this structure.

In order to demonstrate the effects of presence of square hole as well as its dimension on the post-buckling behavior of plate Fig. 4 is portrayed. It can be understood from this figure that rise of the magnitude of this hole can lead to decrement of post-buckling load. Clearly, because stiffness

of structure tends to decrease.

The variations of dimensionless post-buckling load as function of deflection amplitude at different elastic foundation are shown in Fig. 5. As observed, existence of surrounding elastic foundation is a must for improvement of the post-buckling behavior of structure. It is because of the fact that the medium results in increase in stiffness of whole structure. Furthermore, shear modulus parameter known as Pasternak foundation plays a paramount role in post-buckling response of plate.

Fig. 6 shows the effect of various amounts of CNT's volume fraction on non-dimensional post-buckling response versus deflection. It is transparent that increment of volume fraction leads to rise of post-buckling load. It is owing to the reason that reinforcing the structure with nanocomposites increases stiffness of whole structure as
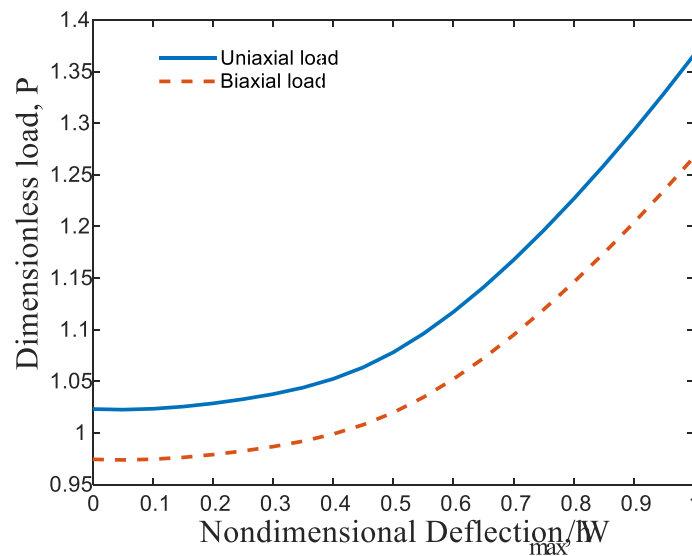
Fig. 8 Effect of both biaxial and uniaxial compressive forces on non-dimensional post-buckling load

well and subsequently amend mechanical properties of plate.

Agglomeration of CNTs on the dimensionless buckling load versus deflection is presented in Fig. 7. It is shown that agglomeration can reduce the buckling load due to instable status in the nanocomposite structure.

The influence of applying both biaxial and uniaxial compressive forces on the post-buckling behavior of structure is illustrated in Fig. 8. As can be seen, applying biaxial compressive load declines post-buckling response of structure. It is obvious that applying biaxial compressive load possesses much more intensity in comparison with uniaxial compressive load and hence, post-buckling response of plate is reduced.

5. Conclusions

Post-buckling analysis of cut out plate reinforced by CNTs resting on elastic medium was carried out. The structure is exposed to biaxial compressive force. Utilizing FSDT as well as Hamilton's principle, motion equations were derived and in the next step using Rayleigh-Ritz method as well as Newton-Raphson iterative technique, the post-buckling response of this structure was achieved and studied. Furthermore, various parameters containing CNT's volume fraction, structure's aspect ratio, cut out measurement, biaxial and uniaxial compressive force and different elastic coefficients and subsequently their effects upon post-buckling response of the plate were elaborately investigated. The obtained outcomes prove that:

- Increment of plate's aspect ratio leads to reduction of post-buckling response.
- Rise of dimension of square hole located at the central domain of plate causes to decrease in the toughness of

plate and therefore, it reduces the post-buckling response.

- Considering an elastic medium including Winkler and Pasternak foundations result in betterment of post-buckling behavior of plate, owing to its effect on the stiffness of whole structure.
- As expected, growth of CNTs volume fraction is one of the essential means for increase in post-buckling load, because reinforcing the plate through nanocomposites increases stiffness of plate and subsequently amend mechanical properties of plate.
- It is shown that agglomeration can reduce the buckling load
- Imposing biaxial compressive load leads to decrease in post-buckling load of structure.

References

Akbas, S.D. (2019), "Post-buckling analysis of a fiber reinforced composite beam with crack", *Eng. Fract. Mech*., **212**, 70-80. https://doi.org/10.1016/j.engfracmech.2019.03.007.

Akgoz, B. and Civalek, O. (2016), "Bending analysis of embedded carbon nanotubes resting on an elastic foundation using strain gradient theory", *Acta. Astronaut*., **119**, 1-12. https://doi.org/10.1016/j.actaastro.2015.10.021.

Asghar, S., Naeem, M.N. and Hussain, M. (2020), "Non-local effect on the vibration analysis of double walled carbon nanotubes based on Donnell shell theory", *Physica E*., **116**, 113726. https://doi.org/10.1016/j.physe.2019.113726.

Do, V.N.V. and Lee, C.H. (2018), "Numerical investigation on post-buckling behavior of FGM sandwich plates subjected to in-plane mechanical compression", *Ocean. Eng*., **170**, 20-42. https://doi.org/10.1016/j.oceaneng.2018.10.007.

Faroughi, S., Rahmani, A. and Friswell, A.I. (2019), "On wave propagation in two-dimensional functionally graded porous rotating nano-beams using a general nonlocal higher-order beam model", *Appl. Math. Model*., In Press.

Gangele, A., Garala, S.K. and Pandey, A.K. (2018), "Influence of

van der Waals forces on elastic and buckling characteristics of vertically aligned carbon nanotubes", *Int. J. Mech. Sci.*, **146-147**, 191-199. https://doi.org/10.1016/j.ijmecsci.2018.07.032.

Gul, U. and Aydogdu, M. (2017), "Wave propagation in double walled carbon nanotubes by using doublet mechanics theory", *Physica E.*, **93**, 345-357. https://doi.org/10.1016/j.physe.2017.07.003.

Herrmann, A.S., Zahlen, P.C. and Zuardy, I. (2005), "Sandwich Structures technology in commercial aviation", *Proceedings of the 7th International Conference on Sandwich Structures*. 13–26, Aalborg, Danmark.

Karimiasl, M., Ebrahimi, F. and Manesh, V. (2020), "On nonlinear vibration of sandwiched polymer- CNT/GPL-fiber nanocomposite nanoshells", *Thin. Wall. Struct.*, **146**, 106431. https://doi.org/10.1016/j.tws.2019.106431.

Kolahchi, R., Hosseini, H., Fakhar, M.H., Taherifar, R. and Mahmoudi, M. (2019), "A numerical method for magneto-hygro-thermal postbuckling analysis of defective quadrilateral graphene sheets using higher order nonlocal strain gradient theory with different movable boundary conditions", *Comput. Math. Appl.*, **78**(6), 2018-2034. https://doi.org/10.1016/j.camwa.2019.03.042.

Kolahdouzan, F., Ghorbanpour Arani, A. and Abdollahian, M. (2018), "Buckling and free vibration analysis of FG-CNTRC-micro sandwich plate", *Steel Compos. Struct.*, **26** (3), 273-287. https://doi.org/10.12989/scs.2018.26.3.273.

Liu, D., Li, Z., Kitipornchai, S. and Yang, J. (2019), "Three-dimensional free vibration and bending analyses of functionally graded graphene nanoplatelets-reinforced nanocomposite annular plates", *Compos. Struct.*, **229**, 111453. https://doi.org/10.1016/j.compstruct.2019.111453.

Moradi-Dastjerdi, R. and Behdinan, K. (2020), "Stability analysis of multifunctional smart sandwich plates with graphene nanocomposite and porous layers", *Int. J. Mech. Sci.*, **167**, 105283. https://doi.org/10.1016/j.ijmecsci.2019.105283.

Ninh, D.G. (2018), "Nonlinear thermal torsional post-buckling of carbon nanotube-reinforced composite cylindrical shell with piezoelectric actuator layers surrounded by elastic medium", *Thin. Wall. Struct.*, **123**, 528-538. https://doi.org/10.1016/j.tws.2017.11.027.

Oktem, A.S. and Adali, S. (2018), "Buckling of shear deformable polymer/clay nanocomposite columns with uncertain material properties by multiscale modeling", *Compos. Part. B-Eng.*, **145**, 226-231. https://doi.org/10.1016/j.compositesb.2018.03.023.

Qin, Z., Zhao, S., Pang, X., Safaei, B. and Chu, F. (2019), "A unified solution for vibration analysis of laminated functionally graded shallow shells reinforced by graphene with general boundary conditions", *Int. J. Mech. Sci.*, In Press.

Vinson, J.R. (1999), "The Behavior of Sandwich Structures of Isotropic and Composite Materials", CRC Press, Boca Raton.

Wang, H., Li, P. and Wu, M. (2019), "Crossarm length optimization and post-buckling analysis of prestressed stayed steel columns", *Thin. Wall. Struct.*, **144**, 106371. https://doi.org/10.1016/j.tws.2019.106371.

Yang, W.D., Fang, C.Q. and Wang, X. (2017), "Nonlinear dynamic characteristics of FG-CNTs reinforced microbeam with piezoelectric layer based on unifying stress-strain gradient framework", *Compos. Part. B-Eng.*, **111**, 372-385. https://doi.org/10.1016/j.compositesb.2016.11.058.

CC